Controls on Arctic sea ice from first-year and multi-year ice survivability

Kyle C. Armour *, Cecilia M. Bitz, and LuAnne Thompson

University of Washington, Seattle, Washington

Elizabeth C. Hunke

Los Alamos National Laboratory, Los Alamos, New Mexico

* *Corresponding author address:* Kyle Armour, Department of Physics, University of Washington, Seattle, WA 98195.

E-mail: karmour@u.washington.edu

ABSTRACT

Recent observations of Arctic sea ice show that the decrease in summer ice cover over the last few decades has occurred in conjunction with a significant loss of multi-year ice. The transition to an Arctic that is populated by thinner, first-year sea ice has important implications for future trends in area and volume. Here, we develop a reduced model for Arctic sea ice with which we investigate how the survivability of first-year and multi-year ice control the mean state, variability, and trends in ice area and volume. A hindcast with a global dynamic-thermodynamic sea ice model that traces first-year and multi-year ice is used to estimate the survivability of each ice type. These estimates of survivability, in concert with the reduced model, yield a persistence time scale of September area and volume anomalies and the characteristics of the sensitivity of sea ice to climate forcing that compare well with a fully coupled climate model. The September area is found to be nearly in equilibrium with climate forcing at all times, and therefore the observed decline in summer sea ice cover is a clear indication of a changing climate. Keeping an account of first-year and multi-year ice area within global climate models offers a powerful way to evaluate those models with observations, and could help to constrain projections of sea ice decline in a warming climate.

1. Introduction

Sea ice can be viewed in two distinct area categories: First-year (FY) ice that was formed since the summer minimum in the previous September and multi-year (MY) ice that has survived at least one summer melt season (see Fig. 1). Recent estimates of the FY and MY ice area by direct observation and by model estimates of sea ice age (Johannessen et al. 1999; Comiso 2002; Rigor and Wallace 2004; Nghiem et al. 2007; Maslanik et al. 2007; Kwok et al. 2009; Hunke and Bitz 2009) invite new perspectives on changing sea ice geometry under greenhouse warming.

Studies of recent Arctic sea ice show that the decrease in area of ice in September (Stroeve et al. 2007; Meier et al. 2007) has been accompanied by a drastic reduction in the area of MY ice in all seasons (Johannessen et al. 1999; Comiso 2002; Nghiem et al. 2007; Maslanik et al. 2007; Kwok et al. 2009). The area reduction has been much larger in summer than winter (Stroeve et al. 2007; Deser and Teng 2008), consistent with the growth of FY ice to replenish much of the area that was formerly MY ice in winter. Because MY ice is thicker and more able to survive the melt season (Maslanik et al. 2007), the transition to FY ice in winter is presumed to have important future implications.

Less obvious is the strong influence of the seasonal partitioning of FY and MY ice types on the response of summer sea ice cover to climate variability and trends. It is quite possible for a given climatological seasonal cycle of total ice area to be composed of very different proportions of FY and MY ice. Therefore knowing the partitioning of FY and MY ice in observations and climate modeling could offer valuable information about future ice loss. To explore this concept further consider the two possible cases illustrated in Fig. 1. In case A

the climatological season cycle of area is almost entirely a result of expanding and retreating FY ice, while the MY ice is nearly unchanging. In contrast, case B has a considerable seasonal cycle in both the MY and FY ice areas.

Now imagine that a climate perturbation in one year were to cause a negative area anomaly at the end of one summer, which would translate into a negative area anomaly in the MY ice the following winter. Because winter anomalies are largely independent of summer anomalies in observations (Blanchard-Wrigglesworth et al. 2010), we can assume FY ice will fill in much of the gap and there will be a positive area anomaly in the FY ice the following winter. If the ice cover is more like case A with low FY ice survival on average, then we expect very little FY ice to survive the following summer, and the negative area anomaly from the previous summer will likely prevail again. In contrast, the survival of FY ice through the end of summer in case B is almost as high as that of MY ice. Thus it matters very little what the partitioning of FY and MY ice is in a given winter, because both types are just as likely to survive the summer, and area anomalies decay relatively quickly.

Systems with high persistence, like case A, recover more slowly from climate perturbations and have relatively higher variability than do systems with low persistence, like case B. Those systems with longer response times also have increased sensitivity to long-term climate forcing than do systems with shorter response times (Hansen et al 1985; Bitz and Roe, 2004). Thus a key question is, do the characteristics of FY and MY ice within the Arctic more closely resemble case A or case B?

In this study, we investigate these basic interactions with the introduction of a reduced sea ice model for area and volume that depends on the survivability of FY and MY ice. We show how the extent to which FY and MY ice survive to summer can control the large-scale

sea ice response to climate forcing, which we verify with a comprehensive sea ice model that is widely used in climate modeling. The separation of sea ice into FY and MY types leads to a useful framework for understanding current and future trends in Arctic sea ice and yields a novel approach for comparing models with observations in order to improve the accuracy of projections of future ice decline.

2. Reduced Sea Ice Model

At any time of the year the sea ice area is given by the sum of FY and MY ice areas. At the end of the melt season, here defined by the day on which the total ice area reaches its minimum value, all FY ice that has survived the summer is promoted to the MY ice category. If f_n is the area of FY ice and m_n the area of MY ice on the day of minimum ice area in September (at the instance before the promotion of FY ice to the MY category), then the total summer minimum ice area is $s_n = f_n + m_n$, where the index n denotes the year. If F_n and M_n are the areas of FY and MY ice, respectively, on the day of maximum ice area in March then the winter maximum area in year n is $W_n = F_n + M_n$.

The time evolution of the summer minimum sea ice area can be described in terms of the survivability of FY and MY ice. On average, the total ice area expands during the growth season (September to March) as FY ice grows over open water, and contracts through the melt season (March to September) as both FY and MY ice melt out (see Fig. 2). We define the *survival ratio* of ice to be the fraction of ice area to survive over key times of the year[1]. For example, the survival ratio of FY ice over the melt season is $\alpha_n = \frac{f_n}{F_n} = \frac{f_n}{W_n - M_n}$.

[1]Though unitless, the survival ratio is sometimes referred to as a *survival rate*.

Because FY ice area is zero at the beginning of the growth season, its survival ratio over the growth season is undefined. The survival ratio of MY ice over the melt season is $\beta_n^m = \frac{m_n}{M_n}$ and over the growth season is $\beta_n^g = \frac{M_n}{s_{n-1}}$, where s_{n-1} is equal to the amount of MY ice at the beginning of the growth season. MY ice area decreases during the growth season—by deformation into ridges and by export to the subpolar seas, where it melts—so β_n^g is less than one. The survival ratio of MY ice from September to September (over both the growth and melt seasons) is then $\beta_n = \beta_n^g \beta_n^m = \frac{m_n}{s_{n-1}}$.

From these definitions of FY and MY ice survival ratios, f_n and m_n can be written:

$$f_n = \alpha_n \left(W_n - \beta_n^g s_{n-1} \right) \tag{1}$$

and

$$m_n = \beta_n^g \beta_n^m s_{n-1}. \tag{2}$$

The total ice area at the summer minimum is then given by the sum of FY and MY ice areas:

$$s_n = \beta_n^g \left(\beta_n^m - \alpha_n \right) s_{n-1} + \alpha_n W_n. \tag{3}$$

This recursion relation shows explicitly how each year's summer minimum ice area is related to that of the previous year, given the FY and MY ice survival ratios (α, β^g and β^m) and winter maximum ice area (W) in that year.

Equations (1) - (3) can be easily extended to describe sea ice volume. If t_n^f and t_n^m are the average thicknesses of FY and MY ice, respectively, at the summer minimum, then the total summer minimum volume is

$$\begin{aligned} v_n &= t_n^f f_n + t_n^m m_n \\ &= \beta_n^g \left(t_n^m \beta_n^m - t_n^f \alpha_n \right) s_{n-1} + t_n^f \alpha_n W_n. \end{aligned} \tag{4}$$

In (1) - (4), which define the reduced sea ice model, the ice survival ratios must be specified in order to determine the time evolution of sea ice area and volume. Here, we use a comprehensive sea ice model that traces FY and MY ice areas in an internally consistent way to estimate the survival ratios and explore these variables.

3. Sea Ice Simulation

We evaluate a simulation of the Los Alamos sea ice model, CICE version 4.0 (Hunke and Lipscomb 2008), to which we have added a FY ice area tracer. The model employs the same grid and much of the sea ice physics from the Community Climate System Model version 3 (CCSM3), including the elastic-viscous plastic dynamics, ice-thickness distribution, snow accumulation, and multi-layer ice and snow thermodynamics. We use the same run as described in Hunke and Bitz (2009) labeled "high albedo", which uses prescribed atmospheric forcing from the Common Ocean Reference Experiments (Core) version 2 (1958-2006, Large and Yeager 2004) with minor modifications as described in Hunke and Bitz (2009). We refer to this run as the "CICE hindcast".

The FY ice area tracer, which is area conserving, keeps an account of all ice that grows from 15 September in one year to the next, when all FY ice is promoted to MY ice and the account is reset to zero (see Fig. 2). We use 15 September as a proxy for the true minimum area, which is not practical to estimate on the fly in a model with synoptic scale variability.

All of our analysis from CICE is on the "satellite era" (1979-2006). The sea ice extent in the CICE hindcast compares well with passive microwave satellite observations over this period (Fig. 3a). The overall magnitude and interannual variability in September and

March extent is captured well, as is the trend in September extent. However, the model does not reproduce the observed trend in winter—likely because the winter ice extent is highly sensitive to the ocean heat flux convergence beneath the ice (Bitz et al. 2005), for which the model uses annually repeating forcing. That is, our simulation does not have ocean circulation changes, which act to enhance Arctic warming in winter (Bitz et al. 2006). The FY and MY ice conditions over the CICE hindcast are summarized in Table 1 and Figs. 2 - 4.

We also use results of present day and 1%/yr CO_2 ramped integrations of CCSM3, whose sea ice has been described previously by Holland et al. (2006) and Bitz et al. (2006). The FY ice area tracer is not yet implemented in CCSM3, so only total Arctic area and volume are used.

4. Results

A number of basic relations between survival ratios and sea ice area and volume can be derived from (1) - (4) and compared with the the results of the CICE hindcast. To do this, each variable in the reduced model is decomposed into equilibrium and perturbation components. For example, the FY ice survival ratio α_n becomes $\alpha_n = \overline{\alpha} + \alpha'_n$. The equilibrium represents the mean state of the sea ice system after fully adjusting to climate forcing. The perturbation represents variability about the mean state. Later we evaluate what is a sufficient period to define the mean state.

a. Equilibrium ice area

If the loss of MY ice area over the course of a year—equal to $\overline{s} - \overline{m}$ or, equivalently, $\left(1 - \overline{\beta^g}\,\overline{\beta^m}\right)\overline{s}$—is exactly balanced by the area of FY ice surviving the melt season—equal to $\overline{f}$—then the total area at the summer minimum remains unchanged and the system is in equilibrium. At equilibrium, (1) - (3) become

$$\overline{f} = \overline{\alpha}\left(\overline{W} - \overline{\beta^g}\overline{s}\right) = \left(1 - \overline{\beta^g}\,\overline{\beta^m}\right)\overline{s}, \tag{5}$$

$$\overline{m} = \overline{\beta^g}\,\overline{\beta^m}\overline{s}, \tag{6}$$

and

$$\frac{\overline{s}}{\overline{W}} = \frac{\overline{\alpha}}{1 - \overline{\beta^g}\left(\overline{\beta^m} - \overline{\alpha}\right)}. \tag{7}$$

The ratio in (7) is of particular importance because $\overline{s}$ and $\overline{W}$ can be readily estimated from passive microwave satellite data. A further useful relation is the ratio of MY to FY ice at the summer minimum as it depends only on the survivability of MY ice from one summer to the next ($\overline{\beta} = \overline{\beta^g}\,\overline{\beta^m}$):

$$\frac{\overline{m}}{\overline{f}} = \frac{\overline{\beta}}{1 - \overline{\beta}}. \tag{8}$$

We can evaluate how well these relations hold with the results of the CICE hindcast. Using 1979-2006 as an example of a mean state, we approximate the equilibrium value of each variable by its average value over that period (see Table 1). The left hand side of (7), $\frac{\overline{S}}{\overline{W}} = 0.374$, is in good agreement with the right hand side, $\frac{\overline{\alpha}}{1-\overline{\beta^g}\left(\overline{\beta^m}-\overline{\alpha}\right)} = 0.368$. The left hand side of (8), $\frac{\overline{m}}{\overline{f}} = 1.60$, agrees well with the right hand side, $\frac{\overline{\beta}}{1-\overline{\beta}} = 1.51$.

The previous paragraph shows that (7) and (8) hold to within a few percent if we approximate the equilibrium of each variable by its mean over 28 years. We will show in the

following section that the area is never long out of equilibrium and the equilibrium area is well estimated by an average over a few years. In addition, we assume that the ice survival ratios are a reflection of Arctic climate, which may contain trends.

We can determine the sensitivity of $\frac{\bar{s}}{\overline{W}}$ to changes in the ice survival ratios by plotting its dependence on $\overline{\alpha}$ and $\overline{\beta}$ as given by (7). This sensitivity, given by the slope of the surface in Fig. 5, depends critically on the location of the mean state in $\overline{\alpha}$-$\overline{\beta}$ space (see Appendix A for full representations of the slopes). In particular, for a given value of $\frac{\bar{s}}{\overline{W}}$, if $\overline{\beta}$ is large and $\overline{\alpha}$ is small (case A on Figs. 5 and 1) then $\frac{\bar{s}}{\overline{W}}$ is very sensitive to changes in the survival ratios. However, if $\overline{\beta}$ and $\overline{\alpha}$ are comparable (case B on Figs. 5 and 1) then $\frac{\bar{s}}{\overline{W}}$ is relatively insensitive to changes in the survival ratios. This poses a challenge for simulating changes to the summer minimum ice area in warming scenarios; there are many combinations of $\overline{\alpha}$, $\overline{\beta^g}$ and $\overline{\beta^m}$ that can provide a realistic simulation of the climatological seasonal cycle of ice area, and each combination has a unique sensitivity to a changing climate. The results of the CICE hindcast are shown in Fig. 2 and by point C on Fig. 5.

Using (5) and (6), we can evaluate the sensitivities of $\overline{f}$ and $\overline{m}$ to changes in the survival ratios (see Appendix A). These sensitivities reflect that if $\overline{\alpha}$ decreases, then $\overline{f}$ decreases because less FY ice survives the summer melt season and $\overline{m}$ decreases because less FY ice is available to replenish the MY ice category each year. If $\overline{\beta^g}$ or $\overline{\beta^m}$ decreases, then $\overline{m}$ decreases because less MY ice survives the growth or melt seasons, respectively, but there is an increase in $\overline{f}$ because more of the Arctic becomes available for FY ice to grow over the winter (see Figs. 3c and 4). In the CICE hindcast, the FY and MY ice survival ratios decrease at comparable rates, resulting in a large reduction of MY ice area while September FY ice area remains relatively constant (Table 1 and Fig. 3b). These trends in FY and MY

ice areas are consistent with recent observations (e.g., Kwok et al. 2009).

The results of the CICE hindcast indicate that the Arctic sea ice system is in a regime where the total summer minimum ice area $\overline{s}$ is more sensitive to changes in $\overline{\beta^m}$ than in $\overline{\beta^g}$ (see Appendix A and consider values from Table 1). This arises because FY ice may grow in place of the MY ice that is lost during the growth season. Also, $\overline{s}$ is more sensitive to changes in $\overline{\alpha}$ than in either $\overline{\beta^g}$ or $\overline{\beta^m}$ (see point C on Fig. 5). This will become increasingly so as the ratio of MY ice area to FY ice area continues to decrease in a warming climate.

b. Equilibrium ice volume

By use of the reduced model, we can relate trends in ice area to trends in ice volume. In equilibrium, the average sea ice thickness at the summer minimum is

$$\begin{aligned} \overline{t} &= \frac{\overline{v}}{\overline{s}} \\ &= \overline{t^f}\left(1 - \overline{\beta^g}\,\overline{\beta^m}\right) + \overline{t^m}\overline{\beta^g}\,\overline{\beta^m}, \end{aligned} \tag{9}$$

and the ice volume is

$$\overline{v} = \frac{\overline{t^f}\,\overline{\alpha}\,\overline{W}}{1 - \overline{\beta^g}\left(\frac{\overline{t^m}}{\overline{t}}\overline{\beta^m} - \frac{\overline{t^f}}{\overline{t}}\overline{\alpha}\right)}. \tag{10}$$

The finding (from (9)) that the average ice thickness $\frac{\overline{v}}{\overline{s}}$ is independent of $\overline{\alpha}$ can be equivalently expressed as $\frac{1}{\overline{v}}\frac{\partial \overline{v}}{\partial \overline{\alpha}} = \frac{1}{\overline{s}}\frac{\partial \overline{s}}{\partial \overline{\alpha}}$, meaning that the fractional decline in volume is equal to the fractional decline in area under decreasing $\overline{\alpha}$. However, for a decrease in either $\overline{\beta^g}$ or $\overline{\beta^m}$ there will be a larger fractional decline in volume than in area provided that $\overline{t^m} > \overline{t^f}$ (see Appendix A). This arises from the larger area loss of the thick, MY ice than the loss of total ice area under a decrease in either of the MY ice survival ratios. Additionally, $\overline{v}$ can decrease due to thinning of ice within the FY and MY categories (Fig. 4), while $\overline{s}$ is

unchanged with respect to changes in $\overline{t^f}$ and $\overline{t^m}$ (at constant FY and MY ice survivability). We therefore expect a larger percent decrease in volume than area under rising greenhouse gas scenarios. This can be seen in the CICE hindcast (from Table 1, v declined at an average rate of -21%/decade while s declined at -11%/decade, with respect to their average values over 1979-2006) as well as in simulations with GCMs (over the 70 years of CO_2 ramping in the CCSM3 simulation, shown in Fig. 6, v declined at an average rate of -16%/decade while s declined at -12%/decade, with respect to their average values over that period).

c. Interannual variability in ice area

We now consider how the mean survivabilities of FY and MY ice—which set the total summer ice area and partitioning between ice types—control the response of the system to interannual climate variability. The deviation of summer minimum ice area from its equilibrium value in year n is

$$\begin{aligned} s'_n &= s_n - \overline{s} \\ &\approx \overline{\beta^g}\left(\overline{\beta^m} - \overline{\alpha}\right) s'_{n-1} + \left(\overline{W} - \overline{\beta^g}\,\overline{s}\right) \alpha'_n \\ &\quad + \overline{\beta^g}\overline{s}\beta_n^{m'} + \left(\overline{\beta^m} - \overline{\alpha}\right) \overline{s}\beta_n^{g'} + \overline{\alpha} W'_n, \end{aligned} \tag{11}$$

where we have dropped terms that are second order in the perturbed quantities[2]. The persistence of area perturbations from one summer s'_{n-1} to the next summer s'_n is regulated

[2]Using the parameters estimated from the CICE hindcast, the terms that are second order in the perturbations are an order of magnitude smaller than the first order terms. While we expect a similar result for the observed sea ice system and GCM simulations of the modern climate, it should be tested in those cases. Because the variability and mean of each variable could change over time, the relative importance of the second order terms must be further evaluated within GCMs under warming scenarios.

by the quantity multiplying s'_{n-1} in (11), which is large when $\overline{\beta^g}$ and $\overline{\beta^m}$ are large and $\overline{\alpha}$ is small. Thus persistence is high when FY ice survivability and MY ice survivability are different from one another (case A in Figs. 1 and 5) and low when they are comparable (case B in Figs. 1 and 5).

To the extent that the perturbations in the survival ratios and the winter maximum area are described by white noise, (11) is equivalent to a 1^{st}-order autoregressive, or AR(1), process (see Appendix B and von Storch and Zwiers (1999) for the properties of these systems). Then the characteristic response time scale, defined as the e-folding time over which the ice retains information about a perturbation in the summer minimum area, is given by

$$\tau_s = -\frac{1 \text{ year}}{\ln\ \overline{\beta^g}\left(\overline{\beta^m} - \overline{\alpha}\right)}. \tag{12}$$

For the CICE hindcast, this time scale as calculated from the average survival ratios (Table 1) is 1.2 years. Because τ_s is relatively small, the area is never out of equilibrium for long and averaging over only a few years is a sufficient approximation to the current equilibrium state.

This time scale can also be estimated directly from the time series of the minimum ice area from the CICE hindcast. If we assume that the minimum area is an AR(1) process then $\tau_s \approx -\frac{1 \text{ year}}{\ln(R)}$, where $R = 0.24$ is the autocorrelation at lag 1 year of the linearly detrended time series. This gives $\tau_s \approx 0.7$ years, which differs slightly from our first estimate because in (12) we ignored the small correlations among the perturbations[3]. Both estimates of the

[3]Statistically insignificant correlations arise between $\beta_n^{m'}$ and s'_{n-1} ($R = -0.22$) and between α'_n and s'_{n-1} ($R = -0.17$). The 95% confidence interval on the time scale as calculated from the lagged autocorrelation of the September area time series is 0 years to 1.7 years, which is consistent with our estimate from (12).

time scale indicate low year-to-year memory in the minimum sea ice area, consistent with observations (Blanchard-Wrigglesworth et al. 2010). We note that although our analysis is limited to the period 1979-2006, our estimate of memory is consistent with the observed (Fetterer et al. 2004, updated 2009) September ice extent in more recent years: following the record minimum extent in 2007, the extent in each subsequent year showed a slight recovery, and by 2009 the extent had recovered to near the long-term linear trend.

We can determine which variables most influence the year-to-year perturbations in the summer minimum ice area by considering the correlation of each variable in (11) with s'_n. After linearly detrending the time series of each variable in the CICE hindcast, we find that W'_n is correlated with s'_n at $R = 0.1$, $\beta_n^{g'}$ at $R = 0.02$, and s'_{n-1} at $R = 0.24$. Because α'_n and $\beta_n^{m'}$ are significantly correlated with each other ($R = 0.63$), we cannot determine which is most responsible for the variations in s'_n. However, together they account for nearly all of the variance in the summer minimum ice area, with α'_n correlated with s'_n at $R = 0.82$ and $\beta_n^{m'}$ at $R = 0.75$. The survival ratios α'_n and $\beta_n^{m'}$ are driven by stochastic weather conditions during the melt season, so it is likely that area anomalies from before about April do not provide predictability for the summer minimum area.

Modeling studies find increasing variability in the summer minimum ice area in a warming climate (Holland et al. 2009; Goosse et al. 2009). From (11), if the average ice survival ratios $\overline{\alpha}$, $\overline{\beta^g}$ and $\overline{\beta^m}$ continue to decline, α'_n will become increasingly dominant in its control of s'_n. From the CICE hindcast, the variance in α' and $\beta^{m'}$ are comparable. It is therefore likely that increasing variability in the survivability of FY ice, as opposed to simply the transition to an Arctic which is dominated by FY ice, is the source of increasing variability in the summer minimum ice area as simulated by GCMs under greenhouse warming.

d. Interannual variability in ice volume

The perturbations in the summer minimum ice volume about its equilibrium value are given by

$$\begin{aligned} v'_n &= v_n - \overline{v} \\ &= \overline{\beta^g} \left(\frac{\overline{t^m}}{\overline{t}} \overline{\beta^m} - \frac{\overline{t^f}}{\overline{t}} \overline{\alpha} \right) v'_{n-1} + \cdots, \end{aligned} \tag{13}$$

where the terms not shown are with respect to the perturbations α'_n, $\beta_n^{g'}$, $\beta_n^{m'}$, W'_n, $t_n^{f'}$, and $t_n^{m'}$. If these perturbations are well approximated by white noise processes, the memory time scale for volume is then

$$\tau_v = -\frac{1 \text{ year}}{\ln \ \overline{\beta^g} \left(\frac{\overline{t^m}}{\overline{t}} \overline{\beta^m} - \frac{\overline{t^f}}{\overline{t}} \overline{\alpha} \right)}, \tag{14}$$

which is longer than that for area (τ_s) provided that $\overline{t^m} > \overline{t^f}$. This longer time scale arises from the fact that the perturbations in the summer minimum ice volume are dominantly controlled by the perturbations in the thicker MY ice, which carries with it the memory of the sea ice anomalies in the previous year. The persistence time scale for volume is likely longer than τ_v because in (14) we have ignored the additional memory of the previous year's volume that arises through the persistence of MY ice thickness anomalies $t_n^{m'}$ (see Bitz et al. (1996) and L'Heveder and Houssais (2001) for autoregressive models of sea ice thickness).

This time scale, estimated from the average values of the variables from the CICE hindcast (Table 1) is ≈ 2.7 years, which is longer than the corresponding estimate for τ_s. The longer memory time scale for volume than area is also apparent in the CCSM3 simulation (over years -150 to 0 in Fig. 6, $\tau_s \approx 1.4$ years and $\tau_v \approx 7.0$ years). Corresponding to this longer memory time scale is the tendency for ice volume to remain out of equilibrium for much longer periods of time than does area. In contrast to ice area, it is difficult to accu-

rately estimate the equilibrium ice volume with an average over even a large number of years in a volume time series, and care must be taken when determining whether a given change in volume over a short period of time necessarily implies a change in the equilibrium state of the system.

5. Discussion

a. The dependence of Arctic sea ice on FY and MY ice survivability

Through the use of a reduced model for Arctic sea ice and a simulation of sea ice conditions over the period 1979-2006, we have explored the ways in which the survival ratios of FY and MY ice control the summer minimum ice area and volume. The results of the CICE hindcast suggest that perturbations in summer minimum FY and MY ice areas are comparable in magnitude, and so contribute about equally to perturbations in the total minimum area (see Fig. 3b). From our perturbation analysis, we found that the variability in summer ice area is dominated by the perturbations in the survival ratios α and β^m, which are governed mostly by stochastic weather noise through the melt season. Therefore, prediction of the summer minimum ice area in a given year depends more on the accurate prediction of weather conditions through the melt season than on the accurate representation of the FY and MY ice area anomalies that exist before the melt season.

Under decreasing ice survival ratios, larger decreases in summer MY ice area than FY ice area will occur (see Fig. 3b and Appendix A). As a result, trends in the total summer ice area are due more to changes in the amount of MY ice surviving the year than to changes

in the amount of FY ice surviving the summer. This is consistent with the trend under decreasing MY ice survival ratios toward an Arctic that is increasingly dominated by FY ice (see (8)). The CICE hindcast also indicates that Arctic sea ice is in a regime where the ice area is particularly sensitive to changes in the FY ice survival ratio $\overline{\alpha}$ (see Fig. 5). It is therefore critical that trends in FY ice and its survivability are observed and modeled accurately.

b. Memory, variability, and mean state sensitivity

We have found that September ice area and volume behave approximately as AR(1) processes. There are several properties of AR(1) systems that are relevant to understanding the current state of the Arctic sea ice system and what changes can be expected in a warming climate. Firstly, systems with long memory time scales recover more slowly from perturbations than do systems with short memory time scales, and therefore exhibit greater variability in response to a forcing of particular variance (see Appendix B). Secondly, systems with longer response times have enhanced sensitivity to long-term forcing compared to systems with shorter response times (Hansen et al. 1985; Bitz and Roe 2004; also see Appendix A).

The relatively short time scale τ_s for Arctic sea ice area, arising from the survival of ice that grows over the winter, corresponds to a mean state that has relatively little variability about its long-term trend and low sensitivity to trends in the ice survival ratios. The persistence time scale for sea ice volume τ_v is longer than that for ice area, contributing to a relatively greater variance in ice volume than area (see Fig. 6). This longer memory time scale for volume corresponds to a greater volume sensitivity than area sensitivity to

trends in the survival ratios (see Appendix A). Relatively larger reductions in ice volume than area have been shown to occur in the CICE hindcast (Table 1), in GCMs (Fig. 6, Gregory et al. 2002), and in observations (Kwok et al. 2009).

Because September ice area—averaged over only a few years—is at all times very nearly in equilibrium, the observed decrease in Arctic sea ice area is a clear indicator of a changing climate. Conversely, the relatively long time scale τ_v implies that September sea ice volume can be out of equilibrium with climate forcing for long periods of time. Thus, while sea ice volume has been shown to be relatively more sensitive to changes in climate forcing than is ice area, its use as an indicator of changing climate conditions is complicated by its long memory time scale—any statistical test for significance of a trend in ice volume is limited by a reduced number of degrees of freedom (Flato 1994).

c. How does changing memory affect the trajectory of sea ice decline?

Given the strong thickness-growth feedback of sea ice (Bitz and Roe 2004)—where in a warming climate we can expect the thicker MY ice to thin at a greater rate than the thinner FY ice—and the fact that the ratio of MY to FY ice entering into the MY ice category each year is decreasing (see (8)), it is likely that the difference between FY and MY ice survival ratios will decrease in a warming climate. If this occurs, the Arctic sea ice system would move toward a regime of decreased memory and decreased sensitivity to climate forcing (consider Fig. 5, or the equations in Appendix A, as $\overline{\beta^g} \to \overline{\alpha}$ and $\overline{\beta^m} \to \overline{\alpha}$). Indeed, a decrease in quantity $\overline{\beta^g}\left(\overline{\beta^m} - \overline{\alpha}\right)$ is seen to occur over the CICE hindcast, implying a reduction in memory and mean state sensitivity over the course of the simulation (see Table 1). The

loss of MY ice in the observed Arctic sea ice system (Johannessen et al. 1999; Comiso 2002; Nghiem et al. 2007; Maslanik et al. 2007; Kwok et al. 2009) suggests that the system may be undergoing a similar decrease in memory.

If the memory time scale and mean state sensitivity of Arctic sea ice decrease sufficiently quickly under a warming climate, a slowing in the rate of area and volume loss could occur. This is consistent with the characteristic trajectory of September sea ice area decline in twenty-first century simulations where the rate of change of Arctic sea ice area decreases late in the simulation despite a continued increase in climate forcing (e.g., Fig. 6). An inflection point in ice decline could also occur if during the warming the ice survival ratios decrease quickly for some time and then slow in their rate of decrease at some later time. It is the interaction between the trends in the survival ratios (the forcing) and the memory time scale (the sensitivity to forcing) that determines the trajectory of ice decline, and further study with a FY ice tracer within fully coupled climate models is needed to determine the exact reason for the inflection point seen in climate simulations. To establish whether we should expect such a trajectory in the observed sea ice system, we should attempt to estimate the mean state and trends in Arctic sea ice survival ratios from observations and compare these with the results of coupled simulations that exhibit such behavior.

The interpretation of sea ice area and volume as AR(1) processes is useful for gaining insight into the current state and recent trends in the Arctic sea ice system. Its use for long-term projections is dependent upon the assumption that the perturbations in FY and MY survivability that force the system continue to be well approximated by white noise.

d. New metrics for improving sea ice projections

Stroeve et al. (2007) compare observed Arctic sea ice trends to the results of the models participating in the Intergovernmental Panel on Climate Change Fourth Assessment Report (IPCC AR4) under the SRES A1B emissions scenario. Of the models with a mean Arctic ice extent within 20% of the observed ice extent over the period 1953-1995, the multi-model mean trend in September ice extent over the period 1979-2006 was $-4.3 \pm 0.3\%$/decade—considerably less than the trend in observations of $-9.1 \pm 1.5\%$/decade over that period. This suggests that while an accurate reproduction of the seasonal cycle of ice extent is necessary, it is not sufficient to reproduce the correct sensitivity to changing climate conditions.

The findings of Stroeve et al. (2007) are consistent with our result that it is possible to accurately model the climatological seasonal cycle of sea ice area and volume without correctly representing the mean state in FY-MY ice area and thickness space (given by $\overline{\alpha}$, $\overline{\beta^g}$, $\overline{\beta^m}$, $\overline{t^f}$ and $\overline{t^m}$) and its corresponding sensitivity to climate forcing (see Figs. 1 and 5). For example, a sea ice model that tends to homogenize FY and MY ice physics by not resolving t^f and t^m effectively lowers the MY ice survival ratio while raising the FY ice survival ratio. Such a model, though it may reproduce the seasonal cycle of ice area, will nonetheless have decreased memory time scales (particularly for volume) and be generally less sensitive to climate forcing. Indeed, two models that are among the most sophisticated (NCAR CCSM3 and UKMO HadGEM) most closely reproduce the observed trend in September Arctic sea ice extent (Stroeve et al. 2007).

If we are to make accurate projections of September sea ice area and volume trends it is important that sea ice models are validated using more than just the observed area and

volume. Given the connection between memory time scale and mean state sensitivity, one metric for models might be to correctly reproduce the variance and lag 1 year autocorrelations from observations of summer minimum ice area and volume. However, given the relatively short time series of observed ice area and volume, there are large uncertainties associated with using these values to estimate the underlying mean state of the sea ice system. A more useful metric for establishing skill in sea ice projections would be the direct comparison of FY and MY ice survival ratios between models and observations. While observations of Arctic sea ice are now available for such a comparison (e.g., Maslanik et al. 2007 and Kwok et al. 2009), the models participating in the IPCC AR4 have not traced FY and MY ice individually. Thus, we have a valuable opportunity to validate models with observations that have not previously been considered in the modeling process.

6. Conclusions

Motivated by recent studies assessing the characteristics of FY and MY sea ice in the Arctic, we have introduced a reduced model for ice area and volume based upon the survivability of FY and MY ice. This model results in a simple picture of summer minimum Arctic sea ice in which its mean state, memory time scale, and sensitivity to climate forcing can be described naturally in terms of the climatological properties FY and MY ice. Through the addition of a FY ice tracer to the sea ice model CICE, we found that small trends in the ice survival ratios explain the decline in total ice area—and the relatively larger loss of MY ice area—over the 1979-2006 hindcast. The simple relations developed here provide a framework with which to interpret changes in observed Arctic FY and MY ice areas as well.

While models agree that increased greenhouse gas concentrations will result in a reduction of Arctic sea ice area and volume, there is much uncertainty in projections of the rate at which this will occur (Stroeve et al. 2007). Given the critical role of sea ice in the Arctic and global climates, it is important that the cause of these uncertainties is understood and that models be improved. Observations of FY and MY ice survivability can place constraints on sea ice climate sensitivity, and provide a benchmark for models to establish confidence in sea ice projections. Enabling GCMs to trace FY and MY ice independently may then provide insight into the reasons for the discrepancies between modeled and observed Arctic sea ice trends, and into what trajectory of ice decline we should expect in a warming climate.

Acknowledgments.

This work was supported by the National Science Foundation under Grant OCE-0256011 (KCA, CMB and LT). ECH was supported by the Climate Change Prediction Program of the Department of Energy's Office of Biological and Environmental Research. We thank Edward Blanchard-Wrigglesworth, Ian Eisenman, Dargan Frierson, Gerard Roe, Harry Stern, and two anonymous reviewers for their helpful suggestions.

APPENDIX A

Equilibrium Sensitivity Analysis

Here we perform an analysis of the sensitivity of the summer minimum ice area and volume with respect to trends in the survival ratios and winter maximum area. The equilibrium summer minimum total, FY, and MY ice areas, and total ice volume are given by (5) - (7) and (10) in the Research Report. We show how each of these changes with respect to changing survival ratios ($\overline{\alpha}$, $\overline{\beta^g}$, $\overline{\beta^m}$) and winter maximum area ($\overline{W}$) in support of the physical explanations provided in the Research Report.

From (5), the change in summer minimum FY ice area is:

$$\begin{aligned}
\frac{\partial \overline{f}}{\partial \overline{W}} &= \left(1 - \overline{\beta^g}\,\overline{\beta^m}\right) \frac{\overline{s}}{\overline{W}} \\
\frac{\partial \overline{f}}{\partial \overline{\alpha}} &= \left(\overline{W} - \overline{\beta^g}\overline{s}\right) \frac{1 - \overline{\beta^g}\,\overline{\beta^m}}{1 - \overline{\beta^g}\left(\overline{\beta^m} - \overline{\alpha}\right)} \\
\frac{\partial \overline{f}}{\partial \overline{\beta^g}} &= -\overline{s} \frac{\overline{\alpha}}{1 - \overline{\beta^g}\left(\overline{\beta^m} - \overline{\alpha}\right)} \\
\frac{\partial \overline{f}}{\partial \overline{\beta^m}} &= -\overline{s} \frac{\overline{\alpha}\overline{\beta^g}^2}{1 - \overline{\beta^g}\left(\overline{\beta^m} - \overline{\alpha}\right)}.
\end{aligned} \tag{A1}$$

These relations show a decrease in $\overline{f}$ under decreasing $\overline{\alpha}$, and an increase in $\overline{f}$ under decreasing $\overline{\beta^g}$ and $\overline{\beta^m}$. The increase in $\overline{f}$ under decreasing MY ice survival ratios arises as FY ice fills in some of the available area as MY ice area decreases.

From (6), the change in summer minimum MY ice area is:

$$\begin{aligned}
\frac{\partial \overline{m}}{\partial \overline{W}} &= \overline{\beta^g}\,\overline{\beta^m}\frac{\overline{s}}{\overline{W}} \\
\frac{\partial \overline{m}}{\partial \overline{\alpha}} &= \left(\overline{W} - \overline{\beta^g}\overline{s}\right)\frac{\overline{\beta^g}\,\overline{\beta^m}}{1-\overline{\beta^g}\left(\overline{\beta^m}-\overline{\alpha}\right)} \\
\frac{\partial \overline{m}}{\partial \overline{\beta^g}} &= \overline{s}\frac{\overline{\beta^m}}{1-\overline{\beta^g}\left(\overline{\beta^m}-\overline{\alpha}\right)} \\
\frac{\partial \overline{m}}{\partial \overline{\beta^m}} &= \overline{s}\frac{\left(1+\overline{\alpha}\overline{\beta^g}\right)\overline{\beta^g}}{1-\overline{\beta^g}\left(\overline{\beta^m}-\overline{\alpha}\right)}.
\end{aligned} \tag{A2}$$

These show a decrease in $\overline{m}$ under decreases in both FY and MY ice survival ratios because a decrease in $\overline{\beta^g}$ or $\overline{\beta^m}$ decreases the amount of MY ice surviving the growth or melt seasons, and a decrease in $\overline{\alpha}$ decreases the amount of FY ice that is promoted to the MY ice category each year.

Comparing (A1) with (A2) shows that under decreases in $\overline{W}$ or $\overline{\alpha}$, the equilibrium areas $\overline{f}$ and $\overline{m}$ decrease in proportion to their respectively values so as to preserve the ratio $\frac{\overline{m}}{\overline{f}}$ (this is consistent with (8), which shows that the ratio $\frac{\overline{m}}{\overline{f}}$ is independent of $\overline{W}$ or $\overline{\alpha}$). If there is more MY ice than FY ice at the summer minimum (corresponding to $\overline{\beta^g}\,\overline{\beta^m} > 0.5$), then there will be a greater loss of MY ice than FY ice due to decreasing $\overline{W}$ or $\overline{\alpha}$. The results of the CICE hindcast show, on average, more MY ice than FY ice in summer (from Table 1, $\overline{\beta} \approx 0.602$). Thus, in the simulation, the Arctic is in a regime where trends in both FY and MY survival ratios result in a greater change in $\overline{m}$ than $\overline{f}$, as seen in Fig. 3b.

From (7), or from the addition of (A1) and (A2), the change in total summer minimum

ice area is:

$$\begin{aligned}
\frac{\partial \overline{s}}{\partial \overline{W}} &= \frac{\overline{s}}{\overline{W}} \\
\frac{\partial \overline{s}}{\partial \overline{\alpha}} &= \left(\overline{W} - \overline{\beta^g}\overline{s}\right) \frac{1}{1 - \overline{\beta^g}\left(\overline{\beta^m} - \overline{\alpha}\right)} \\
\frac{\partial \overline{s}}{\partial \overline{\beta^g}} &= \overline{s} \frac{\overline{\beta^m} - \overline{\alpha}}{1 - \overline{\beta^g}\left(\overline{\beta^m} - \overline{\alpha}\right)} \\
\frac{\partial \overline{s}}{\partial \overline{\beta^m}} &= \overline{s} \frac{\overline{\beta^g}}{1 - \overline{\beta^g}\left(\overline{\beta^m} - \overline{\alpha}\right)}.
\end{aligned} \tag{A3}$$

From these relations, a change of $\overline{W}$ acts to maintain the ratio $\frac{\overline{s}}{\overline{W}}$ as this ratio depends only on the FY and MY ice survival ratios (see (7)). Also, $\overline{s}$ is more sensitive to changes in $\overline{\beta^m}$ than in $\overline{\beta^g}$ because the value $\overline{\beta^m} - \overline{\alpha}$ is smaller than $\overline{\beta^g}$ (from Table 1, $\overline{\beta^m} - \overline{\alpha} \approx 0.585$ and $\overline{\beta^g} \approx 0.764$). This arises from the ability of FY ice to grow in place of MY ice that is lost during the growth season. As $\overline{s}$ decreases, $\overline{s}$ will become increasingly sensitive to changes in $\overline{\alpha}$ since there will be more FY ice at the beginning of the melt season. Because $\overline{\beta^m} > \overline{\alpha}$, the loss of MY ice area is greater than the gain of FY ice area under decreasing MY ice survival ratios, resulting in a decrease in total ice area.

From (10) and (A3) the change in total ice volume V_{eq} can be related to the change in total ice area $\overline{s}$:

$$\begin{aligned}
\frac{1}{\overline{v}}\frac{\partial \overline{v}}{\partial \overline{W}} &= \frac{1}{\overline{s}}\frac{\partial \overline{s}}{\partial \overline{W}} \\
\frac{1}{\overline{v}}\frac{\partial \overline{v}}{\partial \overline{\alpha}} &= \frac{1}{\overline{s}}\frac{\partial \overline{s}}{\partial \overline{\alpha}} \\
\frac{1}{\overline{v}}\frac{\partial \overline{v}}{\partial \overline{\beta^g}} &= \frac{1}{\overline{s}}\frac{\partial \overline{s}}{\partial \overline{\beta^g}} + \frac{\overline{t^m} - \overline{t^f}}{\overline{t}}\overline{\beta^m} \\
\frac{1}{\overline{v}}\frac{\partial \overline{v}}{\partial \overline{\beta^m}} &= \frac{1}{\overline{s}}\frac{\partial \overline{s}}{\partial \overline{\beta^m}} + \frac{\overline{t^m} - \overline{t^f}}{\overline{t}}\overline{\beta^g}.
\end{aligned} \tag{A4}$$

The fractional change in volume V_{eq} is equal to the fractional change in $\overline{s}$ under changes in $\overline{W}$ and $\overline{\alpha}$, leaving the average thickness unchanged. This results from the fact that changes in $\overline{W}$ and $\overline{\alpha}$ act to preserve the ratio (9) of thick MY ice to thin FY ice (given by

(8)). However, changes in either of the MY ice survival ratios act to change V_{eq} and $\overline{s}$ by fractionally different amounts, where this difference is due to the the fact that the thick MY ice (with thickness $\overline{t^m}$) changes in area by a larger amount than does the thin FY ice (with thickness $\overline{t^f}$). Therefore, there is always a greater fractional loss of ice volume than ice area (and a corresponding thinning of the total average ice thickness) under decreasing MY ice survival ratios, provided that a difference in thickness exists between the FY and MY ice categories.

APPENDIX B

Relevant Properties of AR(1) systems

Here we list several properties of AR(1) systems for use in comparing to our relations for the summer minimum ice area and volume. For additional details and derivations, see von Storch and Zwiers (1999).

An AR(1) process is one of the form

$$x_t = \gamma x_{t-\Delta t} + c + \epsilon_t, \tag{B1}$$

where x_t is the value of variable x at time t, $x_{t-\Delta t}$ is its value at the previous timestep $(t - \Delta t)$, c is a constant, and ϵ_t is white noise (with zero mean and variance σ_ϵ^2). The parameter γ defines the memory of the system, or how much the value of x at each timestep depends on its value at the previous timestep.

The variable x can be separated into its equilibrium and perturbation components as was done in the Research Report (for example, $x_t = x_{eq} + x'_t$). This gives

$$x_{eq} = \frac{c}{1-\gamma}, \tag{B2}$$

and

$$x'_t = \gamma x'_{t-\Delta t} + \epsilon_t. \tag{B3}$$

The variance in x about its equilibrium value is given by

$$\sigma_x^2 = \frac{\sigma_\epsilon^2}{1-\gamma^2}. \tag{B4}$$

The memory time scale (e-folding time scale over which perturbations in x persist, on average) is given by

$$\tau = -\frac{\Delta t}{\ln(\gamma)}. \tag{B5}$$

Equations (B1) - (B5) can be compared with their corresponding relations derived for the summer minimum ice area and volume in the Research Report.

REFERENCES

Bitz, C. M., D. S. Battisti, R. E. Moritz, and J. A. Beesley, 1996: Low-frequency variability in the arctic atmosphere, sea ice, and upper-ocean climate system. *Journal of Climate*, **9**, 394–408.

Bitz, C. M., P. R. Gent, R. A. Woodgate, M. M. Holland, and R. Lindsay, 2006: The influence of sea ice on ocean heat uptake in response to increasing co2. *Journal of Climate*, **19**, 2437–2450.

Bitz, C. M., M. M. Holland, E. C. Hunke, and R. Moritz, 2005: Maintenance of the sea-ice edge. *Journal of Climate*, **18**, 2903–2921.

Bitz, C. M. and G. H. Roe, 2004: A mechanism for the high rate of sea-ice thinning in the arctic ocean. *Journal of Climate*, **17**, 3622–3631.

Blanchard-Wrigglesworth, E., K. C. Armour, C. M. Bitz, and E. DeWeaver, 2010: Persistence of arctic sea ice in a gcm ensemble and observations. *submitted to Journal of Climate*.

Comiso, J. C., 2002: A rapidly declining perennial sea ice cover in the arctic. *Geophysical Research Letters*, **29**, doi:10.1029/2002GL015650.

Deser, C. and H. Teng, 2008: Recent trends in arctic sea ice and the evolving role of atmospheric circulation forcing, 1979-2007, in arctic sea ice decline: observations, projections, mechanisms, and implications. *Arctic Sea Ice Decline*, E. DeWeaver, C. M. Bitz, and

B. Tremblay, Eds., American Geophysical Union, No. 180 in AGU Geophysical Monograph Series, 7–26.

Fetterer, F., K. Knowles, W. Meier, and M. Savoie, 2004, updated 2009: Sea ice index. *Boulder, CO: National Snow and Ice Data Center. Digital media.*

Flato, G. M., 1994: Spatial and temporal variability of arctic ice thickness. *Annals of Glaciology*, **21**, 323–329.

Goosse, H., O. Arzel, C. M. Bitz, A. de Montety, and M. Vancoppenolle, 2009: Increased variability of the arctic summer ice extent in a warmer climate. *Geophysical Research Letters*, **36**, L23702, doi:10.1029/2009gl040546.

Gregory, J. M., P. A. Stott, D. J. Cresswell, N. A. Rayner, C. Gordon, and D. M. H. Sexton, 2002: Recent and future changes in arctic sea ice simulated by the hadcm3 aogcm. *Geophysical Research Letters*, **29**, doi:10.1029/2001GL014575.

Hansen, J., G. Russel, A. Lacis, I. Fung, D. Rind, and P. Stone, 1985: Climate response times: Dependence on climate sensitivity and ocean mixing. *Science*, **229**, 857–859.

Holland, M. M., C. M. Bitz, E. C. Hunke, W. H. Lipscomb, and J. L. Schramm, 2006: Influence of the sea ice thickness distribution on polar climate in ccsm3. *Journal of Climate*, **19**, 2398–2414.

Holland, M. M., C. M. Bitz, L. B. Tremblay, and D. A. Bailey, 2009: The role of natural versus forced change in future rapid summer arctic ice loss. *Arctic Sea Ice Decline: Observations, Projections, Mechanisms, and Implications, Geophys. Monogr. Ser.*, **180**, 133–150.

Hunke, E. C. and C. M. Bitz, 2009: Age characteristics in a multidecadal arctic sea ice simulation. *Journal of Geophysical Research*, **114**, C08013, doi:10.1029/2008JC005186.

Hunke, E. C. and W. H. Lipscomb, 2008: Cice: The los alamos sea ice model, documentation and software user's manual, version 4.0. *Tech. Rep. LA-CC-06-012, Los Alamos National Laboratory, Los Alamos, New Mexico.*

Johannessen, O. M., E. V. Shalina, and M. W. Miles, 1999: Satellite evidence for an arctic sea ice cover in transformation. *Science*, **286**, 1937–1939.

Kwok, R., M. Cunningham, I. G. Rigor, J. H. Zwally, and D. Yi, 2009: Thinning and volume loss of the arctic ocean sea ice cover: 2003-2008. *Journal of Geophysical Research*, **114**, C07005, doi:10.1029/2009JC005312.

Large, W. and S. Yeager, 2004: Diurnal to decadal global forcing for ocean and sea-ice models: The data sets and flux climatologies. *NCAR Tech. Note NCAR/TN-460+STR, CGD Division of the National Center for Atmospheric Research.*

L'Heveder, B. and M. N. Houssais, 2001: Investigating the variability of the arctic sea ice thickness in response to a stochastic thermodynamic atmospheric forcing. *Climate Dynamics*, **17**, 107–125.

Maslanik, J. A., C. Fowler, J. Stroeve, S. Drobot, J. Zwally, D. Yi, and W. Emery, 2007: A younger, thinner arctic ice cover: Increased potential for rapid, extensive sea-ice loss. *Geophysical Research Letters*, **34**, L24501, doi:10.1029/2007GL032043.

Meier, W. N., J. Stoeve, and F. Fetterer, 2007: Whither arctic sea ice? a clear signal

of decline regionally, seasonally, and extending beyond the satellite record. *Annals of Glaciology*, **46**, 428–434.

Nghiem, S. V., I. G. Rigor, D. K. Perovich, P. Clemente-Colón, J. W. Weatherly, and G. Neumann, 2007: Rapid reduction of arctic perennial sea ice. *Geophysical Research Letters*, **34**, L19504, doi:10.1029/2007GL031138.

Rigor, I. G. and J. M. Wallace, 2004: Variations in the age of arctic sea-ice and summer sea-ice extent. *Geophysical Research Letters*, **31**, L09401, doi:10.1029/2004GL019492.

Stroeve, J., M. M. Holland, W. N. Meier, T. Scambos, and M. Serreze, 2007: Arctic sea ice decline: Faster than forecast. *Geophysical Research Letters*, **44**, L09501, doi:10.1029/2007GL029703.

von Storch, H. and F. W. Zwiers, 1999: Statistical analysis in climate research. *Cambridge University Press*.

List of Tables

TABLE 1. Definitions of variables for the reduced sea ice model, with their mean values and linear trends (per decade) from the 1979-2006 CICE hindcast. All variables refer to the northern hemisphere total. Ice areas are in $10^6\,\mathrm{km}^2$, thicknesses in m, volumes in $10^{12}\,\mathrm{m}^3$. Time scales are in years and survival ratios are unitless. The values for v and t are September averages, and the values for t^f and t^m are our best estimate over the CICE hindcast. The values of τ_s and τ_v are calculated by use of (12) and (14), respectively.

variable	definition	mean	trend
s	Total summer minimum area	5.62	−0.62
f	FY summer minimum area	2.16	−0.12
m	MY summer minimum area	3.46	−0.50
W	Total winter maximum area	15.04	−0.15
F	FY winter maximum area	10.66	0.34
M	MY winter maximum area	4.38	−0.48
α	FY melt season survival ratio	0.203	−0.017
β^g	MY growth season survival ratio	0.764	−0.007
β^m	MY melt season survival ratio	0.788	−0.028
β	MY Sep-to-Sep survival ratio ($= \beta^g\beta^m$)	0.602	−0.026
v	Total summer minimum volume	13.52	−2.87
t	Avg summer minimum thickness	2.34	−0.26
t^f	FY avg summer minimum thickness	1.5	
t^m	MY avg summer minimum thickness	3	
τ_s	Persistence time scale for Sep area	1.2	
τ_v	Persistence time scale for Sep volume	2.7	

List of Figures

5 Plot of $\frac{\overline{s}}{\overline{W}} \approx \frac{\overline{\alpha}}{1-\overline{\beta}+\overline{\alpha}\sqrt{\overline{\beta}}}$, which is (7) under the approximation $\overline{\beta^g} \approx \overline{\beta^m} \approx \sqrt{\overline{\beta^g}\,\overline{\beta^m}} = \sqrt{\overline{\beta}}$ (from Table 1, the survival ratios of MY ice through the growth season and melt season are similar), over the regime $\overline{\alpha} < \sqrt{\overline{\beta}}$. Points **A-C** denote different regions on the surface with the same value of $\frac{\overline{s}}{\overline{W}}$ but different values of $\overline{\alpha}$ and $\overline{\beta}$. Point **C** is the result of the CICE hindcast 28 year mean ($\overline{\alpha} = 0.203$ and $\overline{\beta} = 0.602$ from Table 1). Point **A** is $\overline{\alpha} \approx 0.1$ and $\overline{\beta} \approx 0.82$. Point **B** is $\overline{\alpha} \approx 0.3$ and $\overline{\beta} \approx 0.36$. 40

6 Arctic September sea ice area and volume from a CCSM3 simulation with 1% per year CO_2 ramping between the years 0 and 70. Two runs are shown over the years 0 to 70. To illustrate the trends under CO_2 ramping, the two runs have been averaged together over this period, and a 20-year running mean has been applied to this average (thick black line). 41

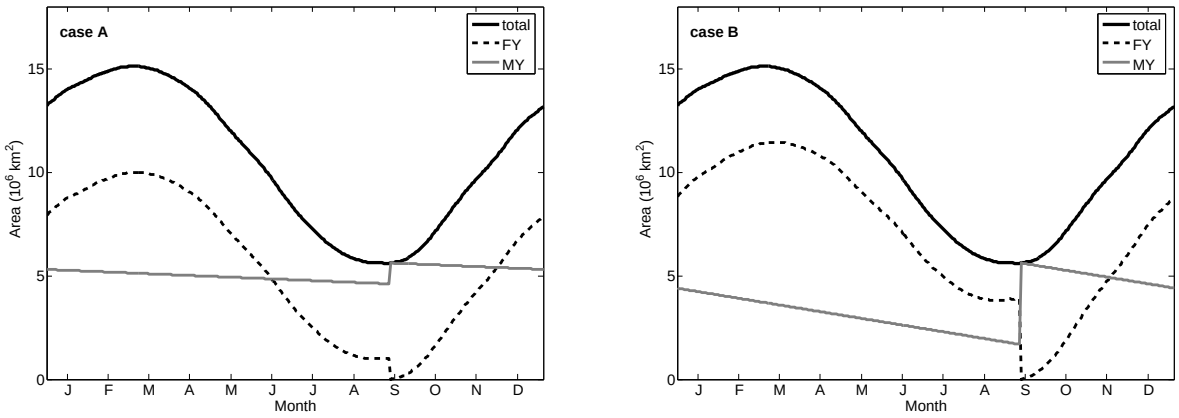

FIG. 1. Sketch showing that the same climatological seasonal cycle of northern hemisphere sea ice area is possible with different proportions of FY and MY ice (the total ice area is equal to the sum of FY and MY ice areas). Case A: FY and MY ice areas consistent with relatively high MY ice survivability and low FY ice survivability. Case B: FY and MY ice areas consistent with relatively low MY ice survivability and high FY ice survivability. At the end of the melt season, defined by the day on which the total ice area reaches its minimum value, all surviving FY ice is promoted to the MY ice category.

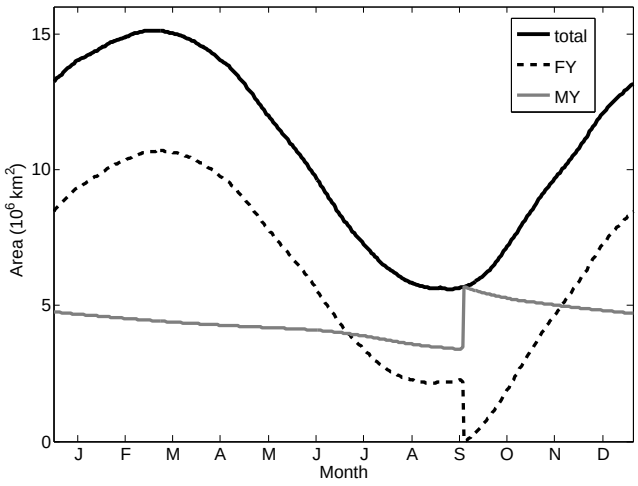

FIG. 2. Seasonal cycle of FY, MY, and total sea ice area for the northern hemisphere from the Los Alamos sea ice model CICE averaged over the period 1979-2006 (see Section 3). In the simulation, FY ice is promoted to the MY ice category on 15 September, at which time the ice area is near its minimum value.

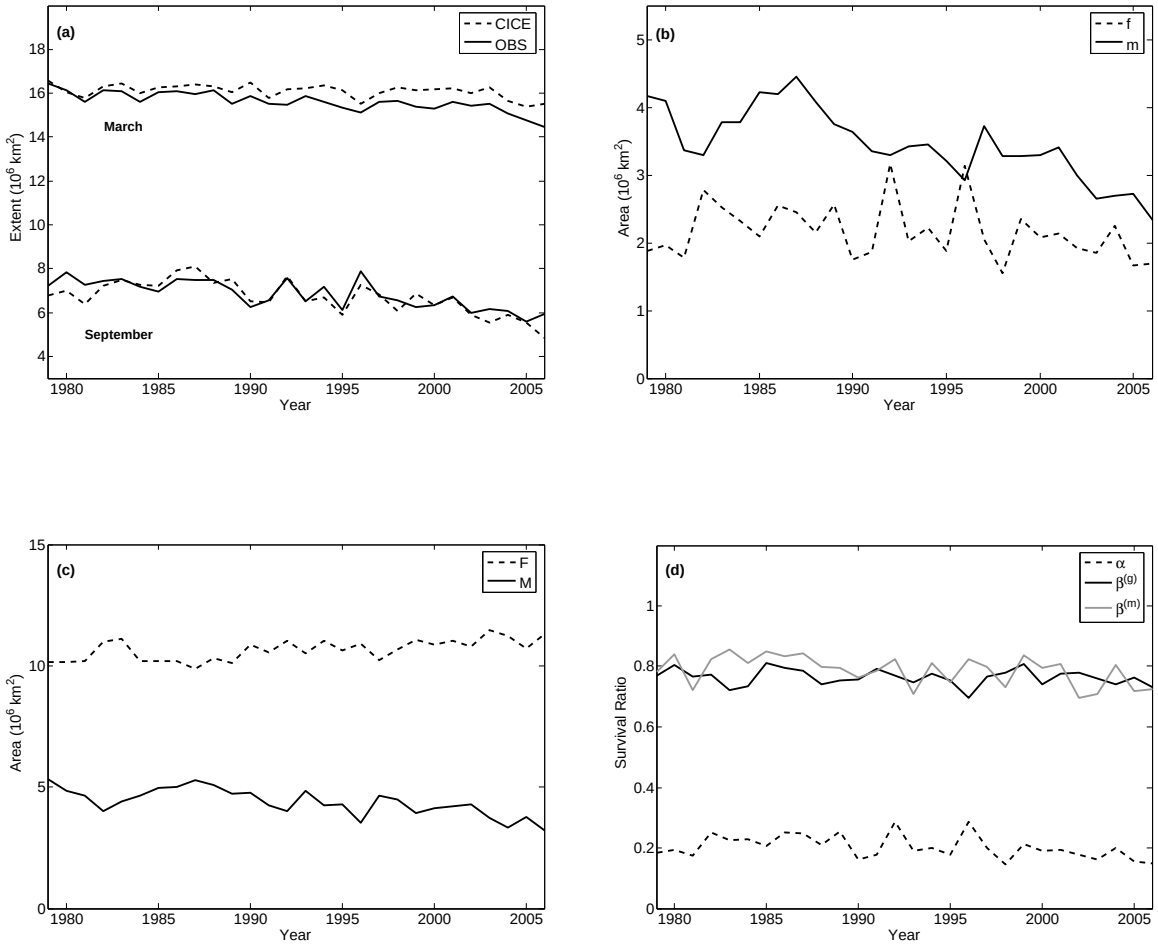

FIG. 3. (a) September and March average ice extent from observations (Fetterer et al. 2004, updated 2009) and the CICE hindcast. (b) 15 September FY (f) and MY (m) ice areas over the CICE hindcast. (c) 15 March FY (F) and MY (M) ice areas over the CICE hindcast. (d) FY and MY ice survival ratios over the CICE hindcast.

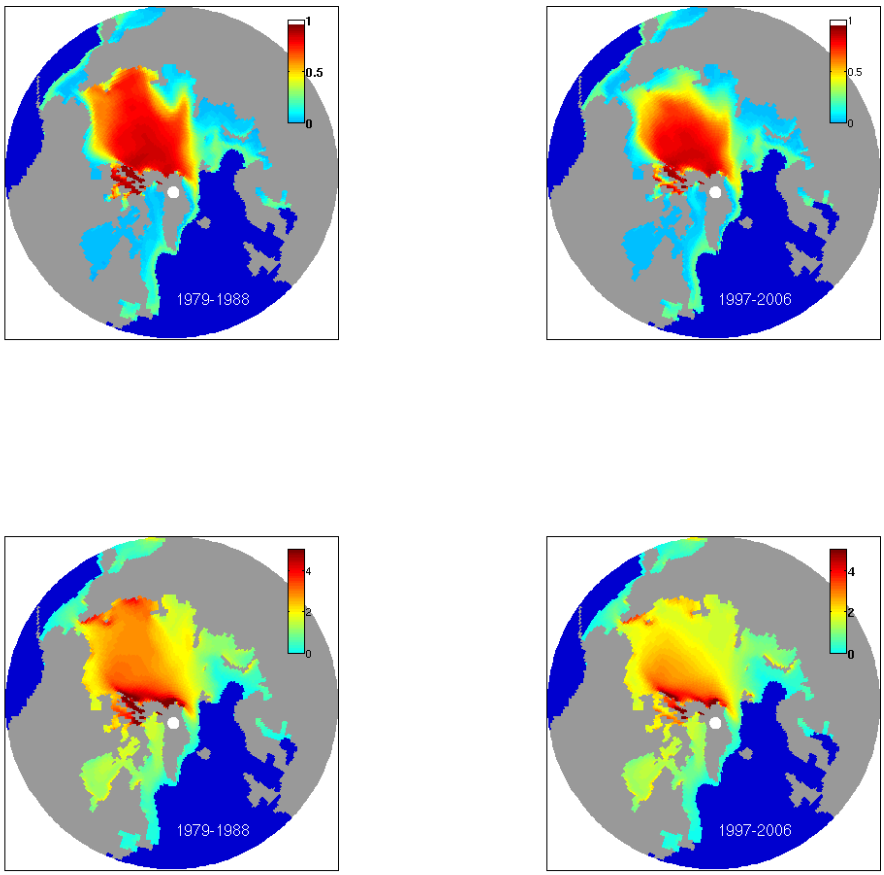

FIG. 4. (Top) 15 March MY ice concentration from the CICE hindcast, averaged over the periods 1979-1998 (left) and 1997-2006 (right). (Bottom) March sea ice thickness (m) from the CICE hindcast, averaged over the periods 1979-1998 (left) and 1997-2006 (right).

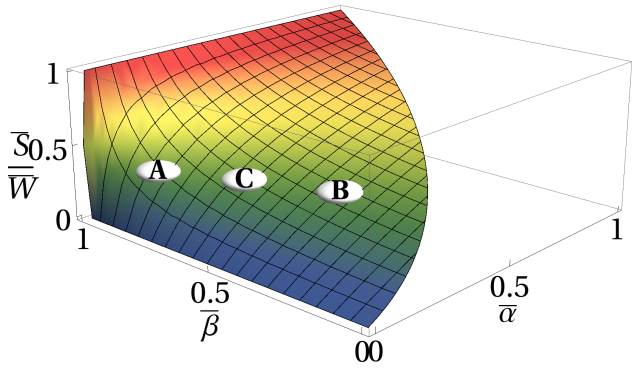

FIG. 5. Plot of $\frac{\overline{s}}{\overline{W}} \approx \frac{\overline{\alpha}}{1-\overline{\beta}+\overline{\alpha}\sqrt{\overline{\beta}}}$, which is (7) under the approximation $\overline{\beta^g} \approx \overline{\beta^m} \approx \sqrt{\overline{\beta^g}\,\overline{\beta^m}} = \sqrt{\overline{\beta}}$ (from Table 1, the survival ratios of MY ice through the growth season and melt season are similar), over the regime $\overline{\alpha} < \sqrt{\overline{\beta}}$. Points **A-C** denote different regions on the surface with the same value of $\frac{\overline{s}}{\overline{W}}$ but different values of $\overline{\alpha}$ and $\overline{\beta}$. Point **C** is the result of the CICE hindcast 28 year mean ($\overline{\alpha} = 0.203$ and $\overline{\beta} = 0.602$ from Table 1). Point **A** is $\overline{\alpha} \approx 0.1$ and $\overline{\beta} \approx 0.82$. Point **B** is $\overline{\alpha} \approx 0.3$ and $\overline{\beta} \approx 0.36$.

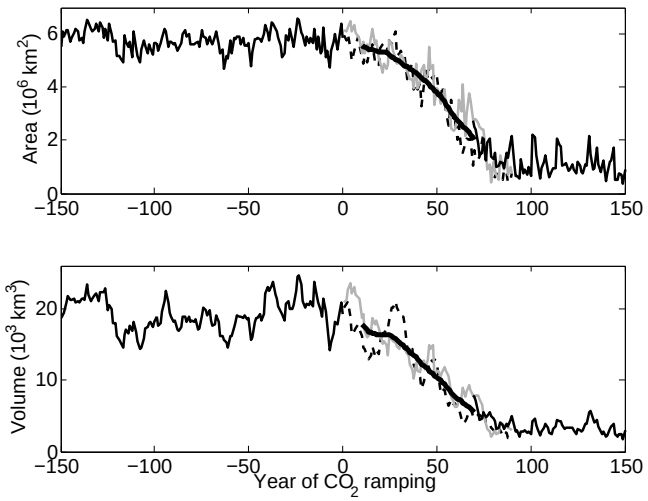

FIG. 6. Arctic September sea ice area and volume from a CCSM3 simulation with 1% per year CO_2 ramping between the years 0 and 70. Two runs are shown over the years 0 to 70. To illustrate the trends under CO_2 ramping, the two runs have been averaged together over this period, and a 20-year running mean has been applied to this average (thick black line).